09

Fourier analysis of modes of microstructured optical fibers

© A.B. Sotsky,[1] D.V. Ponkratov,[1] L.I. Sotskaya[2]

[1] Mogilev State A. Kuleshov University,
212022 Mogilev, Belarus
[2] Belarusian-Russian University,
212000 Mogilev, Belarus
e-mail: ab_sotsky@mail.ru

Received June 14, 2022
Revised August 1, 2022
Accepted August 12, 2022

An vectorial mode solver for microstructured optical fibers based on the representation of the longitudinal components of the mode fields at the interfaces of media in the fiber cross section by Fourier series in angular variables is formulated. The coefficients of the series are found from a homogeneous algebraic system solved by the reduction method. The matrix elements of the system are determined on the basis of the Green's theorem, which is considered in the internal and external regions of the fiber cross section and the inclusions that form the microstructure. The elements are represented by regular integrals, i.e. difficulties associated with the singularities of the Green's functions are absent. The applicability of the approach is limited only by the requirement that the contours of the inclusions and the outer boundary of the fiber are described by single-valued functions of the angular variables. In the special case of a circular dielectric waveguide, the method gives an exact analytical solution of the waveguide problem. Estimates are obtained for the internal convergence of the method in computing the modes of a dielectric elliptical waveguide and microstructural fibers with elliptical inclusions. It is established that the attenuation coefficients of the modes caused by radiation leakage from the fiber core are significantly affected by both the internal microstructure and the outer fiber boundary.

Keywords: microstructured fiber, Green's theorem, Fourier series, internal convergence, leaky modes.

DOI: 10.21883/TP.2022.12.55202.156-22

Introduction

Microstructural optical fibers (MOFs), the cross section of which contains a system of dielectric inclusions, are widely used in optical communication and information processing systems. To optimize such fibers, efficient methods for analyzing their mode characteristics are needed. MOF modes do not allow a rigorous analytical calculation. Therefore, numerical methods are of great practical importance, making it possible to obtain a successively refined solution of the vector waveguide problem [1]. At the present time, in the theory of open dielectric waveguides, which include MOFs, variational and finite-difference methods have become widespread [1]. Their common feature is the use of a computational window limited in space. This makes it difficult to study the modes of open waveguides located in the vicinity of critical and supercritical conditions. The latter conditions take place in the presence of radiation leak from the waveguide channel and are characteristic for MOFs. These limitations can be eliminated by the method of contour integral equations [1–4] and the method of Green's functions [5]. The latter method includes the multipole method [6,7] and the method using Rayleigh series for the electromagnetic field components inside and outside the waveguide channel [8]. In these approaches, the components of the electromagnetic field of the mode at the interfaces between the media, or in closed regions of space are required, and the correct asymptotics of the field with increasing distance from the waveguide is provided by the two-dimensional Green's function. However, in the numerical solution of contour integral equations, difficulties arise due to the singularity of the Green's function. Various ways to overcome these difficulties are discussed in [1–4]. As applied to MOFs, the corresponding results were obtained without taking into account the interaction of their modes with the outer boundary of fiber, which can significantly affect the attenuation of the modes [5,9,10]. This limitation can be overcome using the Green's function method [5]. This method is based on solving systems of equations of coupled waves with respect to the amplitudes of the Fourier expansions of the components of mode electromagnetic field by angular coordinates in the regions of inclusions. But it is effective only for MOFs containing inclusions with circular symmetry [5]. If this symmetry is violated, the above expansions are not absolutely convergent. This gives rise to the asymptotic nature of the obtained solution, which manifests itself in the instability of the results for the mode characteristics with respect to the order of reduction of the Fourier series. Besides, the Green's function method is applicable to a limited class of MOFs whose cross-section contains only elements that can be enclosed in non-intersecting circles [5].

In this paper, we propose a more efficient analogue of the Green's function method. It uses Fourier polynomials by angular coordinates for the longitudinal components of the MOF mode field, given at the boundaries of inclusions

and the outer boundary of the fiber. The amplitudes of the Fourier harmonics are found from a homogeneous algebraic system. Its matrix elements are determined on the basis of Green's theorem, considered in turn in all homogeneous regions of the structure. The calculation of matrix elements is reduced to the numerical calculation of integrals of regular functions, and there are no difficulties caused by the singularities of the Green's functions. A formulation of the dispersion equation for MOF modes is obtained, which does not require direct calculation of the system determinant, which makes it possible to avoid exceeded word length of the computer. The method applicability is limited only by the requirement that the contours of the channel generatrices and the outer boundary of the MOFs are described by single-valued functions of the angular coordinates. In the particular case of a homogeneous fiber with a circular cross-section, the method results in the well-known rigorous solution of the waveguide problem. The internal convergence of the method with respect to the order of the Fourier polynomials was estimated using the examples of calculating the modes of a dielectric waveguide with elliptical cross-section and the MOF modes formed by elliptical air channels in quartz glass. The dispersion dependences for the modes of the elliptical waveguide are compared with the literature data. The effects of modal birefringence and dichroism caused by the radiation leak from the waveguide channel and the influence of the fiber outer boundary on these effects are studied for the MOF.

1. Modes Fourier analysis

The cross-section of the considered fibers is shown schematically in Fig. 1.

The outer boundary of the MOF is closed and is described by single-valued function $r = \rho_0(\varphi)$, where r and φ are global polar coordinates ($x = r\cos\varphi$, $y = r\sin\varphi$) with origin 0 (Fig. 1). Media are considered non-magnetic with relative magnetic permeability $\mu = 1$. The MOF environment is homogeneous and has a relative permittivity ε_c. Inside MOF (region $r < \rho_0(\varphi)$) there are inclusions with numbers $k = \overline{1, N}$ surrounded by homogeneous medium with permittivity ε_s. The media inside the inclusions are also homogeneous. The permittivity of the kth inclusion is equal to ε_k ($k = \overline{1, N}$). The boundary of the inclusion is closed and is described by the single-valued function $r_k = \rho_k(\varphi)$, where r_k and φ_k are polar coordinates of the point in the local coordinate system of the inclusion. It is assumed that the origin of the k-th inclusion, which has global Cartesian coordinates x_{0k}, y_{0k}, can be enclosed in some circle of radius $a_k < \rho_k(\varphi_k)$, entirely located inside the inclusion (Fig. 1). The permittivities $\varepsilon_c, \varepsilon_s, \varepsilon_k$ ($k = \overline{1, N}$) are generally complex.

All components of the mode field with dependence from time t and coordinate z in the form $\exp(i\omega t - ik_0\beta z)$ ($k_0 = 2\pi/\lambda$ — vacuum wavenumber, β — dimensionless mode propagation constant) propagating along the waveguide axis 0z, can be expressed in terms of the longitudinal components of this field E_z and H_z [11], which throughout the space comply with the equations

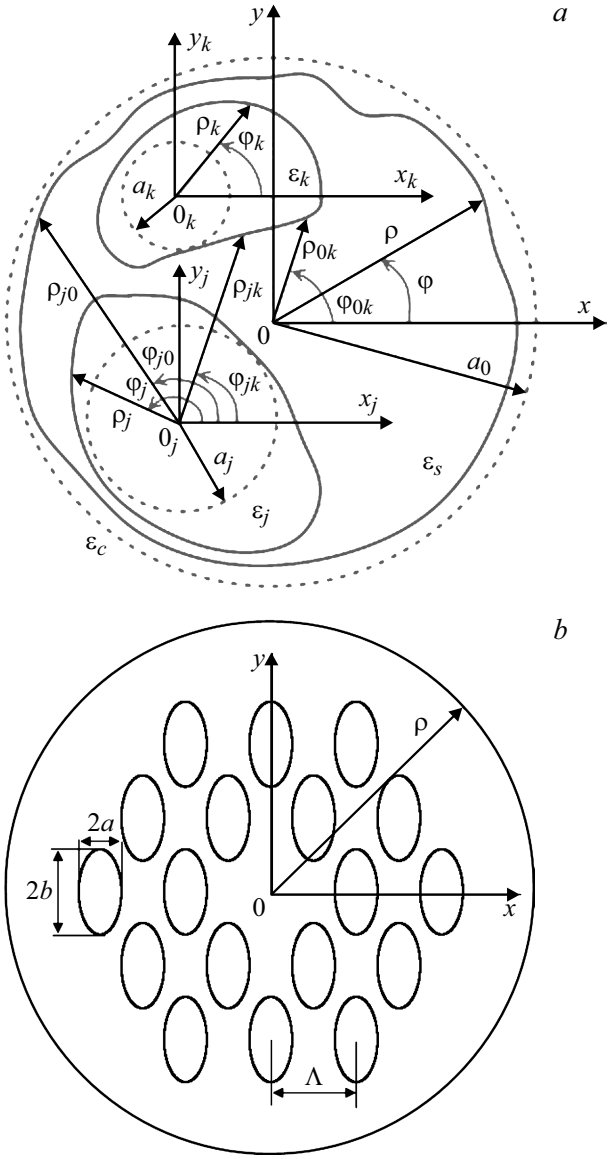

Figure 1. *a* — general view of the cross-section of the studied fibers, *b* — MOF with elliptical air channels.

$$\frac{\partial^2 E_z}{\partial x^2} + \frac{\partial^2 E_z}{\partial y^2} + k_0^2\chi^2 E_z = f_1, \tag{1}$$

$$\frac{\partial^2 H_z}{\partial x^2} + \frac{\partial^2 H_z}{\partial y^2} + k_0^2\chi_s^2 H_z = f_2, \tag{2}$$

where

$$f_1 = -\frac{\chi^2}{\varepsilon\varepsilon_0}\left\{\frac{k_0\beta}{\omega}\left[\frac{\partial\chi^{-2}}{\partial x}\frac{\partial H_z}{\partial y} - \frac{\partial\chi^{-2}}{\partial y}\frac{\partial H_z}{\partial x}\right]\right.$$

$$\left. + \frac{\partial(\varepsilon\varepsilon_0\chi^{-2})}{\partial x}\frac{\partial E_z}{\partial x} + \frac{\partial(\varepsilon\varepsilon_0\chi^{-2})}{\partial y}\frac{\partial E_z}{\partial y}\right\} - k_0^2(\varepsilon - \varepsilon_s)E_z,$$

$$f_2 = -\frac{k_0\beta}{\omega\mu_0}\left[\frac{\partial\chi^{-2}}{\partial y}\frac{\partial E_z}{\partial x} - \frac{\partial\chi^{-2}}{\partial x}\frac{\partial E_z}{\partial y}\right]$$
$$- \frac{\partial\chi^{-2}}{\partial x}\frac{\partial H_z}{\partial x} - \frac{\partial\chi^{-2}}{\partial y}\frac{\partial H_z}{\partial y} - k_0^2(\varepsilon - \varepsilon_s)H_z,$$

$\chi_s^2 = \varepsilon_s - \beta^2$, $\chi^2 = k_0^2(\varepsilon - \beta^2)$, ε_0 and μ_0 are dielectric and magnetic permeability of vacuum, relative permittivity of space $\varepsilon(x, y)$ is a step function of coordinates.

Applying Green's theorem [12] to equations (1), (2) in the domain $r < \rho_0(\varphi)$ according to the scheme described in [5], leads to functional equations

$$\int_0^{2\pi} d\varphi' \sqrt{\rho_0'^2 + \rho_0^2}\left[\Phi_l(\mathbf{r}')\frac{\partial G_s}{\partial n'} - G_s\frac{\partial\Phi_l(\mathbf{r}')}{\partial n'}\right]_{r'=\rho_0(\varphi')-0}$$
$$- \sum_{k=1}^{N}\int_0^{2\pi} d\varphi_k' \sqrt{\rho_k'^2 + \rho_k^2}$$
$$\times\left[\Phi_l(\mathbf{r}')\frac{\partial G_s}{\partial n'} - G_s\frac{\partial\Phi_l(\mathbf{r}')}{\partial n'}\right]_{r_k'=\rho_k(\varphi_k')+0} = 0 \qquad (3)$$

and quadrature formulas

$$\int_0^{2\pi} d\varphi' \sqrt{\rho_0'^2 + \rho_0^2}\left[\Phi_l(\mathbf{r}')\frac{\partial G_s}{\partial n'} - G_s\frac{\partial\Phi_l(\mathbf{r}')}{\partial n'}\right]_{r'=\rho_0(\varphi')-0}$$
$$- \sum_{k=1}^{N}\int_0^{2\pi} d\varphi_k' \sqrt{\rho_k'^2 + \rho_k^2}$$
$$\times\left[\Phi_l(\mathbf{r}')\frac{\partial G_s}{\partial n'} - G_s\frac{\partial\Phi_l(\mathbf{r}')}{\partial n'}\right]_{r_k'=\rho_k(\varphi_k')+0} = \Phi_l(\mathbf{r}). \qquad (4)$$

Here

$$l = 1, 2,\ \Phi_1 = H_z, \quad \Phi_2 = \bar{E_z} = \sqrt{\varepsilon_0/\mu_0}E_z,$$
$$\rho_0' = (d\rho_0/d\varphi)_{\varphi=\varphi'}, \quad \rho_0 = \rho_0(\varphi'),$$
$$\rho_k' = (d\rho_k/d\varphi_k)_{\varphi_k=\varphi_k'}, \quad \rho_k = \rho_k(\varphi_k'),$$
$$G_s = 0.25iH_0^{(2)}(k_0\chi_s|\mathbf{r} - \mathbf{r}'|),$$

— two-dimensional Green's function for a homogeneous medium with permittivity ε_s ($H_0^{(2)}(\ldots)$ — Hankel function), $\mathbf{r}$ and $\mathbf{r}'$ are radius vectors of observation points and integration contours, respectively; r', φ' are polar coordinates of the radius vector $\mathbf{r}'$ in the global coordinate system, r_k', φ_k' are polar coordinates of the same vector in local coordinate systems of inclusions ($k = \overline{1, N}$); $\partial/\partial n'$ denote derivatives by the directions of external perpendiculars to the integration contours. Equations (3) are valid if the point of observation $\mathbf{r}$ is located either in the regions of inclusions or outside the MOF ($r > \rho_0(\varphi)$), and (4) — if this point is located inside the MOF ($r < \rho_0(\varphi)$), but outside the inclusions.

Similarly, applying Green's theorem to equations (1), (2) in the MOF environment and in the internal regions of inclusions, we obtain

$$\int_0^{2\pi} d\varphi' \sqrt{\rho_0'^2 + \rho_0^2}\left[\Phi_l(\mathbf{r}')\frac{\partial G_c}{\partial n'} - G_c\frac{\partial\Phi_l(\mathbf{r}')}{\partial n'}\right]_{r'=\rho_0(\varphi')+0} = 0$$
$$\big(r < \rho_0(\varphi)\big), \qquad (5)$$

$$\int_0^{2\pi} d\varphi' \sqrt{\rho_0'^2 + \rho_0^2}\left[\Phi_l(\mathbf{r}')\frac{\partial G_c}{\partial n'} - G_c\frac{\partial\Phi_l(\mathbf{r}')}{\partial n'}\right]_{r'=\rho_0(\varphi')+0}$$
$$= -\Phi_l(\mathbf{r}) \quad \big(r > \rho_0(\varphi)\big), \qquad (6)$$

where $G_c = 0.25iH_0^{(2)}(k_0\chi_c|\mathbf{r} - \mathbf{r}'|)$, $\chi_c = \sqrt{\varepsilon_c - \beta^2}$, $\operatorname{Re}\chi_c > 0$ and $\operatorname{Im}\chi_c < 0$ for leaking and waveguide MOF modes, respectively;

$$\int_0^{2\pi} d\varphi_k' \sqrt{\rho_k'^2 + \rho_k^2}\left[\Phi_l(\mathbf{r}')\frac{\partial G_k}{\partial n'} - G_k\frac{\partial\Phi_l(\mathbf{r}')}{\partial n'}\right]_{r'=\rho_k(\varphi_k')-0} = 0$$
$$\big(r_k < \rho_k(\varphi_k)\big), \qquad (7)$$

$$\int_0^{2\pi} d\varphi_k' \sqrt{\rho_k'^2 + \rho_k^2}\left[\Phi_l(\mathbf{r}')\frac{\partial G_k}{\partial n'} - G_k\frac{\partial\Phi_l(\mathbf{r}')}{\partial n'}\right]_{r'=\rho_k(\varphi_k')-0}$$
$$= \Phi_l(\mathbf{r}) \quad \big(r_k > \rho_k(\varphi_k)\big), \qquad (8)$$

where $G_k = 0.25iH_0^{(2)}(k_0\chi_k|\mathbf{r} - \mathbf{r}'|)$, $\chi_k = \sqrt{\varepsilon_k - \beta^2}$, $k = \overline{1, N}$.

In order to algebraize equations (3), (5), (7) we represent the functions $\Phi_l(\mathbf{r}')$ and $\partial\Phi_l(\mathbf{r}')/\partial n'$ on integration contours in the form of Fourier polynomials:

$$H_z\big|_{r_k'=\rho_k} = \sum_{\nu=-m}^{m} h_\nu^{(k)}\exp(i\nu\varphi_k'),$$
$$\bar{E_z}\big|_{r_k'=\rho_k} = \sum_{\nu=-m}^{m} e_\nu^{(k)}\exp(i\nu\varphi_k'), \qquad (9)$$
$$\left.\frac{\partial H_z}{\partial n'}\right|_{r'=\rho_k-0} = \sum_{\nu=-m}^{m} h_\nu'^{(k)}\exp(i\nu\varphi_k'),$$
$$\left.\frac{\partial\bar{E_z}}{\partial n'}\right|_{r'=\rho_k-0} = \sum_{\nu=-m}^{m} e_\nu'^{(k)}\exp(i\nu\varphi_k'), \qquad (10)$$
$$H_z\big|_{r'=\rho_0} = \sum_{\nu=-m}^{m} h_\nu^{(0)}\exp(i\nu\varphi'),$$
$$\bar{E_z}\big|_{r'=\rho_0} = \sum_{\nu=-m}^{m} e_\nu^{(0)}\exp(i\nu\varphi'), \qquad (11)$$
$$\left.\frac{\partial H_z}{\partial n'}\right|_{r'=\rho_0+0} = \sum_{\nu=-m}^{m} h_\nu'^{(0)}\exp(i\nu\varphi'),$$

$$\left.\frac{\partial \bar{E}_z}{\partial n'}\right|_{r'=\rho_0+0} = \sum_{\nu=-m}^{m} e_\nu'^{(0)} \exp(i\nu\varphi'), \tag{12}$$

where m — order of polynomials, $h_\nu^{(k)}$, $h_\nu'^{(k)}$, $e_\nu^{(k)}$, $e_\nu'^{(k)}$ — unknown coefficients ($k = \overline{0, N}$).

Note that, in accordance with the Graph addition theorem for cylindrical functions [13]:

$$H_0^{(2)}(\kappa|\mathbf{r}-\mathbf{r}'|) = \sum_{\mu=-\infty}^{\infty} \exp[i\mu(\varphi-\varphi')] \times \begin{cases} J_\mu(\kappa r) H_\mu^{(2)}(\kappa r') & \text{at } r < r', \\ J_\mu(\kappa r') H_\mu^{(2)}(\kappa r) & \text{at } r > r', \end{cases} \tag{13}$$

where κ — some constant, $J_\mu(\ldots)$ — Bessel function; r, φ and r', φ' — polar coordinates of the radius vectors $\mathbf{r}$ and $\mathbf{r}'$ in some coordinate system, and that the projection of the gradient vectors of the Hankel functions onto the directions of the perpendiculars to the integration contours in (3)–(8) leads to the relations

$$\frac{\partial G_{s,c}}{\partial n'} = \left(\rho_0 \frac{\partial G_{s,c}}{\partial r'} - \frac{\rho_0'}{\rho_0}\frac{\partial G_{s,c}}{\partial \varphi'}\right)_{r'=\rho_0} (\rho_0'^2 - \rho_0^2)^{-0.5}, \tag{14}$$

$$\frac{\partial G_{s,k}}{\partial n'} = \left(\rho_k \frac{\partial G_{s,k}}{\partial r_k'} - \frac{\rho_k'}{\rho_k}\frac{\partial G_{s,k}}{\partial \varphi_k'}\right)_{r_k'=\rho_k} (\rho_k'^2 - \rho_k^2)^{-0.5}. \tag{15}$$

Formulas (5), (7), (13)–(15) make it possible to establish a relationship between the expansion coefficients (9)–(12). Indeed, let us describe a certain circle of radius $a < \rho_0(\varphi)$ around the origin of the global coordinate system 0. As follows from (5), (11), (12), (14), within this circle

$$\sum_{\mu=-\infty}^{\infty} J_\mu(k_0\chi_c r)\exp(i\mu\varphi) \sum_{\nu=-m}^{m} \left(K_{\mu\nu}^{(0)} h_\nu^{(0)} + L_{\mu\nu}^{(0)} h_\nu'^{(0)}\right) = 0, \tag{16}$$

where

$$K_{\mu\nu}^{(0)} = \int_0^{2\pi} d\varphi' \Big\{ k_0\chi_c\rho_0 H_\mu'^{(2)}(k_0\chi_c\rho_0) + i\mu\frac{\rho_0'}{\rho_0} H_\mu^{(2)}(k_0\chi_c\rho_0)\exp[i(\nu-\mu)\varphi'] \Big\}, \tag{17}$$

$$L_{\mu\nu}^{(0)} = \int_0^{2\pi} d\varphi' \sqrt{\rho_0'^2+\rho_0^2}\, H_\mu^{(2)}(k_0\chi_c\rho_0)\exp[i(\nu-\mu)\varphi'], \tag{18}$$

$H_\mu'^{(2)}(\ldots)$ denotes the derivative of the Hankel function $H_\mu^{(2)}(\ldots)$ with respect to each of arguments. Considering that the functions $J_\mu(k_0\chi_c r)\exp(i\mu\varphi)$ in (16) related to different μ are linearly independent and limited in the external sum in (16) by terms with $\mu = \overline{-m, m}$ we conclude that

$$h_\nu'^{(0)} = \sum_{\mu=-m}^{m} Z_{\nu\mu}^{(0)} h_\mu^{(0)}, \tag{19}$$

where

$$Z_{\nu\mu}^{(0)} = \sum_{\sigma=-m}^{m} L_{\nu\sigma}^{(0)-1} K_{\sigma\mu}^{(0)},$$

$\mathbf{L}^{(0)-1}$ — matrix inverse to the matrix $\mathbf{L}^{(0)}$ of the form (18). Similarly

$$e_\nu'^{(0)} = \sum_{\mu=-m}^{m} Z_{\nu\mu}^{(0)} e_\mu^{(0)}. \tag{20}$$

Similar transformations of equations (7) considering (9), (10), (13), (15) lead to the relations

$$h_\nu'^{(k)} = \sum_{\mu=-m}^{m} Z_{\nu\mu}^{(k)} h_\mu^{(k)}, \tag{21}$$

$$e_\nu'^{(k)} = \sum_{\mu=-m}^{m} Z_{\nu\mu}^{(k)} e_\mu^{(k)}, \tag{22}$$

$$Z_{\nu\mu}^{(k)} = \sum_{\sigma=-m}^{m} L_{\nu\sigma}^{(k)-1} K_{\sigma\mu}^{(k)}, \tag{23}$$

$$K_{\mu\nu}^{(k)} = \int_0^{2\pi} d\varphi_k' \Big\{ k_0\chi_k\rho_k J_\mu'(k_0\chi_k\rho_k) + i\mu\frac{\rho_k'}{\rho_k} J_\mu(k_0\chi_k\rho_k)\exp[i(\nu-\mu)\varphi_k'] \Big\}, \tag{24}$$

$$L_{\mu\nu}^{(k)} = \int_0^{2\pi} d\varphi_k' \sqrt{\rho_k'^2+\rho_k^2}\, \{J_\mu(k_0\chi_k\rho_k)\exp[i(\nu-\mu)\varphi_k']\}, \tag{25}$$

where $J_\mu'(\ldots)$ denotes the derivative of the function $J_\mu(\ldots)$ with respect to each of arguments, $k = \overline{1, N}$.

Let us now review equations (3). The derivatives $\partial H_z/\partial n'$ and $\partial \bar{E}_z/\partial n'$ entering into them differ from the analogous derivatives in (10) and (12) in that they are calculated striving to the interface of media from opposite sides. It follows from the continuity conditions for the tangential components of the electric and magnetic fields at these interfaces that

$$\left(\frac{\partial H_z}{\partial n'}\right)_{r'=\rho-0} = \frac{\chi_s^2}{\chi_c^2}\left(\frac{\partial H_z}{\partial n'}\right)_{r'=\rho+0} + \frac{\beta}{\sqrt{\rho'^2+\rho^2}} \times \left(1-\frac{\chi_s^2}{\chi_c^2}\right)\left(\frac{\partial \bar{E}_z}{\partial \varphi'}\right)_{r'=\rho}, \tag{26}$$

$$\left(\frac{\partial \bar{E}_z}{\partial n'}\right)_{r'=\rho-0} = \frac{\chi_s^2\varepsilon_c}{\chi_c^2\varepsilon_s}\left(\frac{\partial \bar{E}_z}{\partial n'}\right)_{r'=\rho+0} - \frac{\beta}{\varepsilon_s\sqrt{\rho'^2+\rho^2}} \times \left(1-\frac{\chi_s^2}{\chi_c^2}\right)\left(\frac{\partial H_z}{\partial \varphi'}\right)_{r'=\rho}, \tag{27}$$

$$\left(\frac{\partial H_z}{\partial n'}\right)_{r'=\rho_k+0} = \frac{\chi_s^2}{\chi_k^2}\left(\frac{\partial H_z}{\partial n'}\right)_{r'=\rho_k-0} + \frac{\beta}{\sqrt{\rho_k'^2+\rho_k^2}} \times \left(1-\frac{\chi_s^2}{\chi_k^2}\right)\left(\frac{\partial \bar{E}_z}{\partial \varphi_k'}\right)_{r'=\rho_k}, \tag{28}$$

$$\left(\frac{\partial \bar{E}_z}{\partial n'}\right)_{r'=\rho_k+0} = \frac{\chi_s^2\varepsilon_k}{\chi_k^2\varepsilon_s}\left(\frac{\partial \bar{E}_z}{\partial n'}\right)_{r'=\rho_k-0} - \frac{\beta}{\varepsilon_s\sqrt{\rho_k'^2+\rho_k^2}} \times\left(1-\frac{\chi_s^2}{\chi_k^2}\right)\left(\frac{\partial H_z}{\partial \varphi_k'}\right)_{r'=\rho_k}. \quad (29)$$

Formulas (26)–(29) allow the expansions (9)–(12) use in equations (3).

Let us detail equations (3) for the case when the observation point with the radius vector $\mathbf{r}$ is in the j-th inclusion. Its polar coordinates in the local coordinate system of the inclusion will be denoted by r_j, φ_j. Let $r_j < a_j$ (Fig. 1). To calculate the functions G_s, $\partial G_s/\partial n'$ on the integration contours in (3), we use the local coordinate system of the j-th inclusion. Denote the polar coordinates of the boundary points of the k-th inclusion by ρ_{jk}, φ_{jk} (if $j=k$, then $\rho_{jk}=\rho_k$, $\varphi_{jk}=\varphi_k'$), and the outer boundary of the MOF is associated with the number $k=0$, so that the polar coordinates of its points are equal to ρ_{j0}, φ_{j0}. It is clear from Fig. 1 that the inequalities $r_j < \rho_{jk}$ $(k=\overline{0,N})$ are met. Then, in accordance with (13), in all integrals in (3):

$$G_s = 0.25i\sum_{\mu=-\infty}^{\infty}\exp[i\mu(\varphi_j-\varphi_{jk})]J_\mu(k_0\chi_s r_j)H_\mu^{(2)}(k_0\chi_s\rho_{jk}). \quad (30)$$

To calculate the derivatives of $\partial G_s/\partial n'$, note that

$$x_{0k}+\rho_k\cos\varphi_k' = x_{0j}+\rho_{jk}\cos\varphi_{jk},$$
$$y_{0k}+\rho_k\sin\varphi_k' = y_{0j}+\rho_{jk}\sin\varphi_{jk}, \quad (31)$$

where $x_{00}=y_{00}=0$, $\varphi_0'=\varphi'$. According to (31):

$$\rho_{jk} = \sqrt{(x_{0k}-x_{0j}+\rho_k\cos\varphi_k')^2+(y_{0k}-y_{0j}+\rho_k\sin\varphi_k')^2}, \quad (32)$$

$$\frac{\partial\varphi_{jk}}{\partial\rho_k} = \frac{(x_{0k}-x_{0j})\sin\varphi_k'-(y_{0k}-y_{0j})\cos\varphi_k'}{\rho_{jk}^2}, \quad (33)$$

$$\frac{\partial\rho_{jk}}{\partial\rho_k} = \frac{(x_{0k}-x_{0j})\cos\varphi_k'+(y_{0k}-y_{0j})\sin\varphi_k'+\rho_k}{\rho_{jk}}, \quad (34)$$

$$\frac{\partial\rho_{jk}}{\partial\varphi_k'} = -\rho_k\rho_{jk}\frac{\partial\varphi_{jk}}{\partial\rho_k}, \quad (35)$$

$$\frac{\partial\varphi_{jk}}{\partial\varphi_k'} = \frac{\rho_k}{\rho_{jk}}\frac{\partial\rho_{jk}}{\partial\rho_k}. \quad (36)$$

As follows from (15), (30)–(36):

$$\frac{\partial G_s}{\partial n'} = \frac{i}{4\sqrt{\rho_k'^2+\rho_k^2}}\sum_{\mu=-\infty}^{\infty}J_\mu(k_0\chi_s r_j)\exp[i\mu(\varphi_j-\varphi_{jk}] \times\left[k_0\chi_s\rho_k H_\mu'^{(2)}(k_0\chi_s\rho_{jk})\left(\frac{\partial\rho_{jk}}{\partial\rho_k}+\frac{\rho_k'\rho_{jk}}{\rho_k}\frac{\partial\varphi_{jk}}{\partial\rho_k}\right)\right. -i\mu H_\mu^{(2)}(k_0\chi_s\rho_{jk})\left.\left(\rho_k\frac{\partial\varphi_{jk}}{\partial\rho_k}-\frac{\rho_k'}{\rho_{jk}}\frac{\partial\rho_{jk}}{\partial\rho_k}\right)\right]. \quad (37)$$

When relations (14), (15), (19), (22), (26)–(30), (37) are taken into account, equations (3) for $l=1,2$ are reduced to form

$$\sum_{\mu=-\infty}^{\infty}J_\mu(k_0\chi_s r_j)\exp(i\mu\varphi_j)\sum_{k=0}^{N}\sum_{\nu=-m}^{m}\left(HH_{\mu\nu}^{(jk)}h_\nu^{(k)} + HE_{\mu\nu}^{(jk)}e_\nu^{(k)}\right)=0, \quad (38)$$

$$\sum_{\mu=-\infty}^{\infty}J_\mu(k_0\chi_s r_j)\exp(i\mu\varphi_j)\sum_{k=0}^{N}\sum_{\nu=-m}^{m}\left(EH_{\mu\nu}^{(jk)}h_\nu^{(k)} + EE_{\mu\nu}^{(jk)}e_\nu^{(k)}\right)=0, \quad (39)$$

where

$$HH_{\mu\nu}^{(jk)} = T1_{\mu\nu}^{(jk)} - \frac{\chi_s^2}{\chi_k^2}\sum_{\sigma=-m}^{m}T2_{\mu\sigma}^{(jk)}Z_{\sigma\nu}^{(k)}, \quad (40)$$

$$EE_{\mu\nu}^{(jk)} = T1_{\mu\nu}^{(jk)} - \frac{\chi_s^2\varepsilon_k}{\chi_k^2\varepsilon_s}\sum_{\sigma=-m}^{m}T2_{\mu\sigma}^{(jk)}Z_{\sigma\nu}^{(k)}, \quad (41)$$

$$HE_{\mu\nu}^{(jk)} = -i\nu\beta\left(1-\frac{\chi_s^2}{\chi_k^2}\right)T3_{\mu\nu}^{(jk)}, \quad (42)$$

$$EH_{\mu\nu}^{(jk)} = \frac{i\nu\beta}{\varepsilon_s}\left(1-\frac{\chi_s^2}{\chi_k^2}\right)T3_{\mu\nu}^{(jk)}, \quad (43)$$

$$T1_{\mu\nu}^{(jk)} = \frac{is_k}{4}\int_0^{2\pi}d\varphi_k'\left[k_0\chi_s\rho_k H_\mu'^{(2)}(k_0\chi_s\rho_{jk})\times\left(\frac{\partial\rho_{jk}}{\partial\rho_k}+\frac{\rho_k'\rho_{jk}}{\rho_k}\frac{\partial\varphi_{jk}}{\partial\rho_k}\right)-i\mu H_\mu^{(2)}(k_0\chi_s\rho_{jk})\times\left(\rho_k\frac{\partial\varphi_{jk}}{\partial\rho_k}-\frac{\rho_k'}{\rho_{jk}}\frac{\partial\rho_{jk}}{\partial\rho_k}\right)\right]\exp(i\nu\varphi_k'-i\mu\varphi_{jk}), \quad (44)$$

$$T2_{\mu\nu}^{(jk)} = \frac{is_k}{4}\int_0^{2\pi}d\varphi_k'\sqrt{\rho_k'^2+\rho_k^2}H_\mu^{(2)}(k_0\chi_s\rho_{jk})\times\exp(i\nu\varphi_k'-i\mu\varphi_{jk}), \quad (45)$$

$$T3_{\mu\nu}^{(jk)} = \frac{is_k}{4}\int_0^{2\pi}d\varphi_k'H_\mu^{(2)}(k_0\chi_s\rho_{jk})\exp(i\nu\varphi_k'-i\mu\varphi_{jk}), \quad (46)$$

$s_k=-1$ at $k>0$, and at $k=0$, $s_k=1$, $\chi_k=\chi_c$, $\varepsilon_k=\varepsilon_c$.

Considering that in the studied region of change r_j the functions $J_\mu(k_0\chi_s r_j)\exp(i\mu\varphi_j)$ related to different μ_s are linearly independent and limited in external sums in (38), (39) by terms with numbers $\mu=\overline{-m,m}$, we receive the algebraic equations

$$\sum_{k=0}^{N}\sum_{\nu=-m}^{m}\left(HH_{\mu\nu}^{(jk)}h_\nu^{(k)}+HE_{\mu\nu}^{(jk)}e_\nu^{(k)}\right)=0, \quad (47)$$

$$\sum_{k=0}^{N}\sum_{\nu=-m}^{m}\left(EH_{\mu\nu}^{(jk)}h_{\nu}^{(k)}+EE_{\mu\nu}^{(jk)}e_{\nu}^{(k)}\right)=0, \qquad (48)$$

where $\mu=\overline{-m,m}$, $j=\overline{1,N}$.

Now let the observation point in (3) be outside the circle of some radius a_0 enclosing the MOF (Fig. 1, *a*). In this case, to specify the functions G_s, $\partial G_s/\partial n'$ on the integration contours in (3), we use the global coordinate system in Fig. 1, *a*. According to (13):

$$G_s=0.25i\sum_{\mu=-\infty}^{\infty}\exp[i\mu(\varphi-\varphi_{0k})]J_{\mu}(k_0\chi_s\rho_{0k})H_{\mu}^{(2)}(k_0\chi_s r), \qquad (49)$$

$$\frac{\partial G_s}{\partial n'}=\frac{i}{4\sqrt{\rho_k'^2+\rho_k^2}}\sum_{\mu=-\infty}^{\infty}H_{\mu}^{(2)}(k_0\chi_s r)\exp[i\mu(\varphi-\varphi_{0k})]$$
$$\times\left[k_0\chi_s\rho_k J_{\mu}'(k_0\chi_s\rho_{0k})\left(\frac{\partial\rho_{0k}}{\partial\rho_k}+\frac{\rho_k'\rho_{0k}}{\rho_k}\frac{\partial\varphi_{0k}}{\partial\rho_k}\right)\right.$$
$$\left.-i\mu J_{\mu}(k_0\chi_s\rho_{0k})\left(\rho_k\frac{\partial\varphi_{0k}}{\partial\rho_k}-\frac{\rho_k'}{\rho_{0k}}\frac{\partial\rho_{0k}}{\partial\rho_k}\right)\right]. \qquad (50)$$

In accordance with (31)–(36) on the outer boundary of the MOF, when calculating the matrix elements of the system (47), (48), one should set $k=0$, $\rho_0=\rho_{00}$, $\varphi_{00}=\varphi_0'=\varphi'$, $\partial\rho_{00}/\partial\rho_0=1$, $\partial\varphi_{00}/\partial\rho_0=0$.

Substituting (49), (50) into (3) results in the equations

$$\sum_{\mu=-\infty}^{\infty}H_{\mu}^{(2)}(k_0\chi_s r)\exp(i\mu\varphi)\sum_{k=0}^{N}\sum_{\nu=-m}^{m}\left(HH_{\mu\nu}^{(0k)}h_{\nu}^{(k)}\right.$$
$$\left.+HE_{\mu\nu}^{(0k)}e_{\nu}^{(k)}\right)=0, \qquad (51)$$

$$\sum_{\mu=-\infty}^{\infty}H_{\mu}^{(2)}(k_0\chi_s r)\exp(i\mu\varphi)\sum_{k=0}^{N}\sum_{\nu=-m}^{m}\left(EH_{\mu\nu}^{(0k)}h_{\nu}^{(k)}\right.$$
$$\left.+EE_{\mu\nu}^{(0k)}e_{\nu}^{(k)}\right)=0. \qquad (52)$$

As in the case of equations (38), (39), from (51), (52) we obtain

$$\sum_{k=0}^{N}\sum_{\nu=-m}^{m}\left(HH_{\mu\nu}^{(0k)}h_{\nu}^{(k)}+HE_{\mu\nu}^{(0k)}e_{\nu}^{(k)}\right)=0, \qquad (53)$$

$$\sum_{k=0}^{N}\sum_{\nu=-m}^{m}\left(EH_{\mu\nu}^{(0k)}h_{\nu}^{(k)}+EE_{\mu\nu}^{(0k)}e_{\nu}^{(k)}\right)=0, \qquad (54)$$

where $\mu=\overline{-m,m}$. The coefficients of algebraic equations (53), (54) have the general form (40)–(43), but now

$$T1_{\mu\nu}^{(0k)}=\frac{is_k}{4}\int_0^{2\pi}d\varphi_k'\left[k_0\chi_s\rho_k J_{\mu}'(k_0\chi_s\rho_{0k})\right.$$
$$\times\left(\frac{\partial\rho_{0k}}{\partial\rho_k}+\frac{\rho_k'\rho_{0k}}{\rho_k}\frac{\partial\varphi_{0k}}{\partial\rho_k}\right)-i\mu J_{\mu}(k_0\chi_s\rho_{0k})$$
$$\left.\times\left(\rho_k\frac{\partial\varphi_{0k}}{\partial\rho_k}-\frac{\rho_k'}{\rho_{0k}}\frac{\partial\rho_{0k}}{\partial\rho_k}\right)\right]\exp(i\nu\varphi_k'-i\mu\varphi_{0k}), \qquad (55)$$

$$T2_{\mu\nu}^{(0k)}=\frac{is_k}{4}\int_0^{2\pi}d\varphi_k'\sqrt{\rho_k'^2+\rho_k^2}\,J_{\mu}(k_0\chi_s\rho_{0k})$$
$$\times\exp(i\nu\varphi_k'-i\mu\varphi_{0k}), \qquad (56)$$

$$T3_{\mu\nu}^{(0k)}=\frac{is_k}{4}\int_0^{2\pi}d\varphi_k'\,J_{\mu}(k_0\chi_s\rho_{0k})\exp(i\nu\varphi_k'-i\mu\varphi_{0k}). \qquad (57)$$

Equations (47), (48), (53), (54) are a homogeneous algebraic system

$$MX=0 \qquad (58)$$

of dimension $n\times n$, where $n=(4m+2)(N+1)$, X — column vector of dimension n, composed of expansion coefficients (9), (11). As it follows from (44)–(46), (55)–(57), the calculation of the matrix elements of the system $HH_{\mu\nu}^{(jk)}$, $HE_{\mu\nu}^{(jk)}$, $EH_{\mu\nu}^{(jk)}$, $EE_{\mu\nu}^{(jk)}$ is reduced to numerical calculation of integrals from regular functions and does not cause fundamental difficulties.

The condition for the existence of non-trivial solutions of the system (58)

$$\det M=0 \qquad (59)$$

is a dispersion equation with respect to possible complex propagation constants of MOF modes β. After solving the dispersion equation, the mode field can be calculated. If the rank of the matrix M is equal to $n-1$, as in the case for all MOFs studied below, then all components of the vector X can be expressed from (58) in terms of one of its components. As a result, up to an arbitrary factor that has the meaning of the mode amplitude, all expansion coefficients (9), (11) will be found. The subsequent calculation of the longitudinal components of the mode field inside MOF and in the MOF environment can be performed using quadrature formulas (4), (6), (8). The lateral components of the mode field can be calculated by differentiating the found longitudinal components [11].

2. Numerical examples

A special case of MOFs are homogeneous dielectric waveguides surrounded by homogeneous media. In such a situation, $N=0$, and the calculation of waveguide modes is reduced to solving a system of equations (53), (54), where $k=N=0$.

The simplest example of homogeneous waveguide is a circular dielectric waveguide. In this case ρ_0 is the waveguide radius, and $\rho_0'=0$. Thanks to the last equality, integrals (17), (18), (55)–(57) are taken analytically, which leads to diagonal matrices

$$Z_{\mu\nu}^{(0)}=\frac{k_0\chi_c H_{\mu}'^{(2)}(k_0\chi_c\rho_0)}{H_{\mu}^{(2)}(k_0\chi_c\rho_0)}\,\delta_{\mu\nu}, \qquad (60)$$

$$T1_{\mu\nu}^{(00)}=0.5\pi i k_0\chi_s\rho_0 J_{\mu}'(k_0\chi_s\rho_0)\delta_{\mu\nu}, \qquad (61)$$

$$T2_{\mu\nu}^{(00)}=0.5\pi i\rho_0 J_{\mu}(k_0\chi_s\rho_0)\delta_{\mu\nu}, \qquad (62)$$

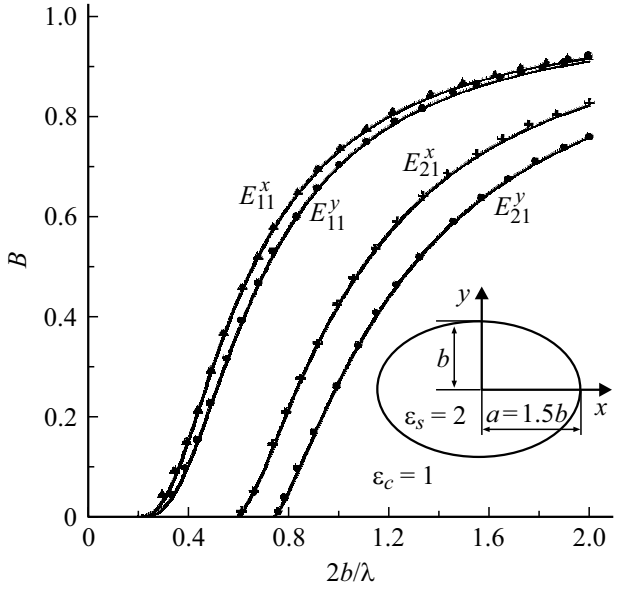

Figure 2. Dispersion dependences for four modes of the lowest order of the elliptical waveguide of $F = a/b = 1.5$ format (insert), calculated by the developed method (solid curves) and obtained in [4] (discrete symbols).

$$T3_{\mu\nu}^{(00)} = 0.5\pi i\, J_\mu(k_0\chi_s\rho_0)\delta_{\mu\nu}, \qquad (63)$$

where $\delta_{\mu\nu}$ — Kronecker symbol. As a result, system (53), (54) splits into unrelated subsystems of two equations relative to $e_\mu^{(0)}$, $h_\mu^{(0)}$, where $\mu = 0, \pm 1, \ldots$. The equal-zero conditions for the determinants of these subsystems lead to the well-known exact dispersion equation for the modes of circular dielectric waveguide [11]. Thus, in this example, the developed method gives a rigorous analytical solution to the waveguide problem.

Another classic example of a homogeneous waveguide is an elliptical dielectric waveguide. In principle, for such waveguide the system of equations (1), (2) allows the separation of variables in elliptic coordinates [14]. But this leads to the difficult problem of the Mathieu functions calculation [13,14]. A detailed calculation of the elliptical waveguide was carried out in [4] by the method of contour integral equations.

In the proposed approach the contour of the cross-section of the elliptical waveguide is described by the functions

$$\rho_0(\varphi) = ab(b^2\cos^2\varphi + a^2\sin^2\varphi)^{-1/2}, \qquad (64)$$

$$\rho_0'(\varphi) = 0.5ab\sin(2\varphi)(b^2 - a^2)(b^2\cos^2\varphi + a^2\sin^2\varphi)^{-3/2}, \qquad (65)$$

where a and b — the lengths of the semi-axes of the ellipse (Fig. 2). As follows from (55)–(57), (64), (65), under the condition $a \neq b$ the matrix M is dense, and the solution of equation (59) can only be found numerically.

In Fig. 2, the dispersion dependences for four modes of the lowest order of the elliptical waveguide of $F = a/b = 1.5$ format, calculated by the above method, are compared with the results of the paper [4]. Here $B = \mathrm{Re}[(\beta^2 - \varepsilon_c)/(\varepsilon_s - \varepsilon_c)]$, and mode designations are used indicating the main transverse component of their electric field [15].

Table 1. Internal convergence of the developed method for elliptical waveguide modes

Mode	E_{11}^x	E_{11}^y	E_{21}^x	E_{11}^y
m	B	B	B	B
4	0.730388	0.699907	0.422658	0.267338
8	0.730520	0.700002	0.423185	0.267904
12	0.730510	0.700012	0.423179	0.267894
16	0.730510	0.700012	0.423178	0.267894
20	0.730510	0.700012	0.423178	0.267894

As can be seen from Fig. 2, the results of both approaches coincide within the graphical errors.

Table 1, which refers to $2b/\lambda = 1$, makes it possible to judge the internal convergence of the proposed method when calculating the curves in Fig. 2.

According to Table 1, the accuracy of calculating the mode propagation constants acceptable for calculations evaluation is already achieved at $m = 4$.

We used the developed method to describe the modal birefringence in MOFs formed by air channels in a dielectric medium. Single-mode fibers with a solid core are considered, in them the inclusion centers are located at the nodes of a two-dimensional hexagonal lattice of period Λ (Fig. 1, *b*). If the inclusions have a circular cross-section, then the MOF cross-section has a rotational symmetry of the order of $s = 6$. In this case, the two orthogonally polarized fundamental MOF modes are degenerate [16], i.e., there is no mode birefringence. This means the instability of the light polarization as it propagates along the fiber, and the occurrence of polarization noise when the optical signal is detected at the MOF output. The elimination of these defects involves the use of fibers with modal birefringence, in which the complex propagation constants of the main orthogonally polarized modes are different [17]. Such situation takes place for MOF with elliptical air channels, when $s = 2$ [5,18,19].

We studied MOFs whose core is surrounded by two hexagonal rings of identical air channels with elliptical cross section of the format $F = a/b$ (Fig. 1, *b*). The contour of the MOF outer boundary was assumed to be circular ($\rho_0 = \mathrm{const}$). The values $N = 18$, $\varepsilon_s = 1.45^2$, $\varepsilon_j = 1$ ($j = \overline{1, N}$) and proportions $\rho_0/\Lambda = 30.85$, $ab/\Lambda^2 = 0.06$, typical for quartz single-mode MOFs [10,20] are used. Two situations are considered when $\varepsilon_c = \varepsilon_c^{(1)} = \varepsilon_s$, i.e. the channels are in an infinite environment and $\varepsilon_c = \varepsilon_c^{(2)} = (1.54 - i0.00002)^2$, which means the presence of absorbing butyl acrylate polymer coating on the fiber [10].

Table 2. Internal convergence of the computational scheme when calculating the propagation constants of MOF modes with circular air channels ($F = 1$) surrounded by a homogeneous medium ($\varepsilon_c = \varepsilon_c^{(11)}$), and if there is a polymer coating on MOF

Modes	H_x			H_y		
ε_c	m	$\mathrm{Re}\,\beta$	$-\mathrm{Im}\,\beta \cdot 10^7$	m	$\mathrm{Re}\,\beta$	$-\mathrm{Im}\,\beta \cdot 10^7$
$\varepsilon_c^{(1)}$	4	1.442991	0.742	4	1.442991	0.742
	8	1.442991	0.743	8	1.442991	0.743
	12	1.442991	0.743	12	1.442991	0.743
$\varepsilon_c^{(2)}$	4	1.442991	0.386	4	1.442991	0.386
	8	1.442991	0.354	8	1.442991	0.354
	12	1.442991	0.354	12	1.442991	0.354

Table 3. Internal convergence of the computational scheme when calculating the propagation constants of MOF modes with elliptical air channels of $F = 1/2$ format surrounded by a homogeneous medium ($\varepsilon_c = \varepsilon_c^{(1)}$), and if there is a polymer coating on MOF ($\varepsilon_c = \varepsilon_c^{(2)}$)

Modes	H_x			H_y		
ε_c	m	$\mathrm{Re}\,\beta$	$-\mathrm{Im}\,\beta \cdot 10^7$	m	$\mathrm{Re}\,\beta$	$-\mathrm{Im}\,\beta \cdot 10^7$
$\varepsilon_c^{(1)}$	4	1.442901	1.469	4	1.442782	0.817
	8	1.442789	0.871	8	1.442659	0.463
	12	1.442770	0.800	12	1.442640	0.424
	16	1.442767	0.786	16	1.442636	0.416
	20	1.442766	0.783	20	1.442635	0.414
	24	1.442766	0.783	24	1.442635	0.414
$\varepsilon_c^{(2)}$	4	1.442901	1.408	4	1.442781	1.943
	8	1.442789	1.731	8	1.442659	0.289
	12	1.442770	1.514	12	1.442640	0.214
	16	1.442767	1.484	16	1.442636	0.203
	20	1.442766	1.478	20	1.442635	0.200
	24	1.442766	1.477	24	1.442635	0.200

Calculations shown that in the case of MOFs the direct numerical solution of equation (59) runs into the problem of the computed values $\det M$ going beyond the computer word length. A similar defect, caused by the multiplication of the set of Hankel functions, was already noted in [5] in the study of MOF with circular inclusions. It can be eliminated by representing the dispersion equation in a form that does not require $\det M$ calculation [5]. For this purpose, system (58) is written in the form

$$\sum_{j \neq k} M_{\nu j} X_j X_k^{-1} = -M_{\nu k} \quad (\nu \neq k), \tag{66}$$

$$\sum_{j=1}^{n} M_{kj} X_j X_k^{-1} = 0, \tag{67}$$

where k — number of one of the equations of system (58). If the determinant of $n-1$-th order of system (66) differs from zero, then this system has a single solution with respect to the unknowns $X_j X_k^{-1}$. Then, after calculating the above quantities from (66) the expression (67) acquires the meaning of the dispersion equation with respect to β. Its solution does not cause fundamental difficulties. Simultaneously, the mode field is determined from (9), (11), (66).

If there are no symmetry elements in the MOF cross-section, then the specific choice of the number k in (66), (67) is not significant. However, if there are symmetry axes in the MOF section, some components of the vector X can become zero [5]. If we take such component as X_k, then the matrix of the system (66) becomes degenerate, and the described scheme loses its meaning. In particular, for the MOFs under study $e_0^{(1)} = 0$, $h_0^{(1)} \neq 0$ when calculating the fundamental mode with the main lateral component of the magnetic field H_x (H_x-mode) and $h_0^{(1)} = 0$, $e_0^{(1)} \neq 0$ when calculating the mode with main component H_y (H_y-mode) [5]. Here number 1 corresponds to the nearest inclusion from the origin, located in the region $x > 0$, the center of which is on the axis $0x$ (Fig. 1, *b*). Therefore, when calculating H_y-mode the component $e_0^{(1)}$ was chosen as X_k, and when calculating H_x-mode — component $h_0^{(1)}$.

Mode birefringence $\mathrm{Re}\,\Delta\beta$, where $\Delta\beta$ — difference of propagation constants of H_x- and H_y-modes and dichroism, i. e., different attenuation of the H_x- and H_y-modes of MOF modes with elliptical air channels are illustrated in Figs 3, 4 and Tables 2, 3.

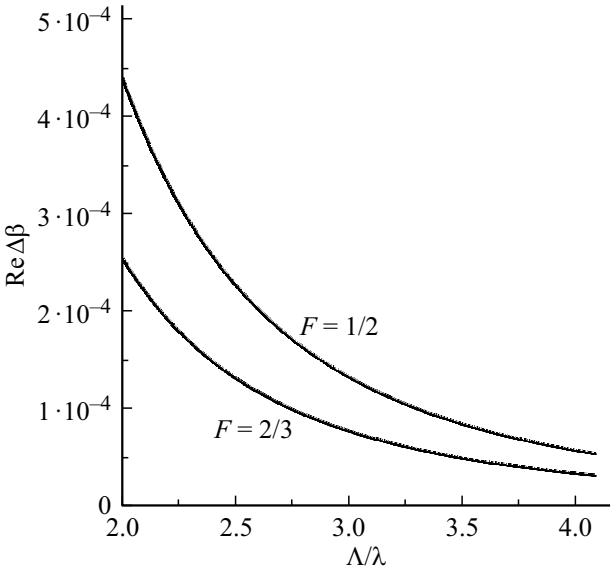

Figure 3. Spectral dependences of the mode birefringence for MOFs with elliptical air channels of 2/3 and 1/2 formats.

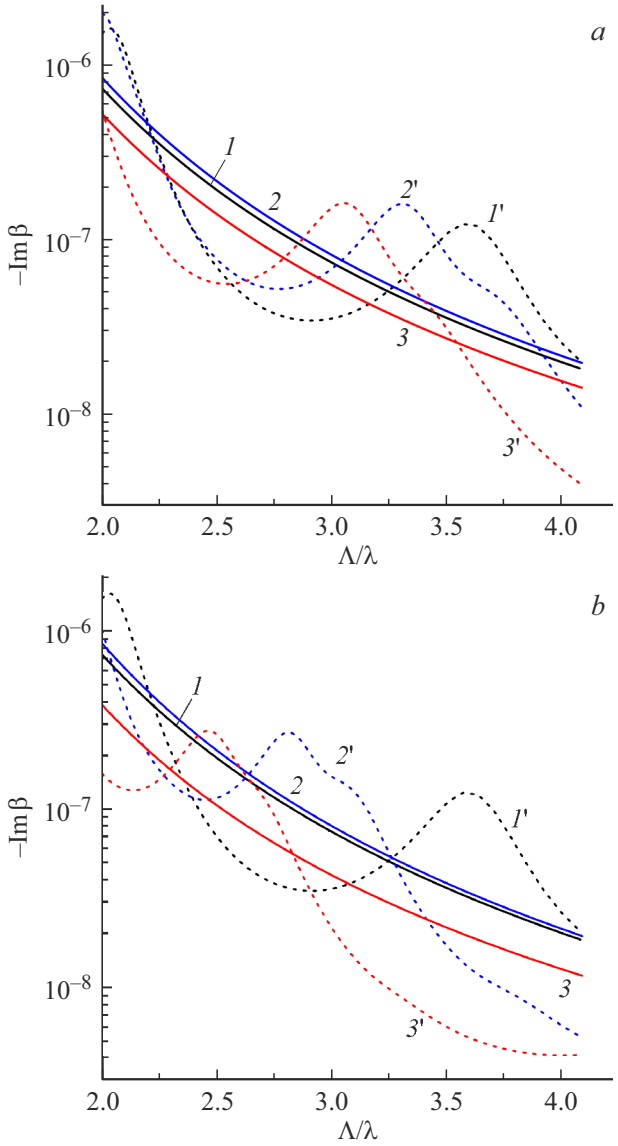

Figure 4. Spectral dependences of damping coefficients of MOF modes with elliptical air channels of the formats $F = 1$ (curves *1*, *1′*), 2/3 (*a*; *2*, *2′* — H_x-mode; *3*, *3′* — H_y-mode) and 1/2 (*b*; *2*, *2′* — H_x-mode; *3*, *3′* — H_y-mode). Curves *1*–*3* — channels in an infinite medium, *1′*–*3′* — MOF with polymer coating.

The curves in Fig. 3 related to $\varepsilon_c = \varepsilon_c^{(1)}$ and $\varepsilon_c = \varepsilon_c^{(1)}$ are indistinguishable within the Figure. According to Fig. 3, the mode birefringence increases with decreasing of ratios F and Λ/λ. Similar patterns were noted in the literature [18,19,21]. In particular, at $\Lambda/\lambda < 2.2$ $\mathrm{Re}\,\Delta\beta$ exceeds $2 \cdot 10^{-4}$, which is typical for conventional fibers with strong stress-induced birefringence [22]. But in MOFs there is also an anisotropy of damping of H_x- and H_y-modes, caused by their radiation leak from the fiber core, which is absent in traditional types of birefringent fibers. The results of calculations by the proposed method of dichroism in the MOFs under consideration are presented in Fig. 4.

Tables 2 and 3 make it possible to judge the internal convergence of the developed method when calculating the dependences in Fig. 3, 4. The data presented in them refer to $\Lambda/\lambda = 3$.

From a comparison of Tables 2 and 3, we can conclude that increase in the format of air channels has a negative effect on the speed of convergence of the computational scheme, which is explained by the complication of the fields configuration described by the Fourier polynomials (9), (11). It also follows from Tables 2 and 3 that the propagation constants of the MOF modes in the form of air channels in infinite quartz glass and MOF modes of the same polarization and with the same air channels, but with a polymer coating have practically the same real parts, however their imaginary parts differ significantly.

In Table 3 and Fig. 3, the closeness of the indicated values $\mathrm{Re}\,\beta$ is explained by the fact that the fields of fundamental MOF modes are well localized in the core of the fiber and weakly interact with the outer boundary of the fiber [5]. At the same time, this interaction leads to the formation of standing waves between the air channels and the boundary $r = \rho_0$, which significantly affects the damping of the modes caused by radiation leak from the fiber core [10]. According to Table 3 this effect leads to increase in mode dichroism, which opens up the possibility of creating the single-mode single-polarization fibers for telecommunication and sensor applications. The resonant nature of this effect [10] leads to nonmonotonic dependences $\mathrm{Im}\,\beta(\lambda)$, shown in Fig. 4 by dashed lines. As follows from Fig. 4, these dependences essentially depend on the internal structure of MOF.

Conclusion

A new method for solving the vector waveguide eigenvalue problem for MOF modes with an arbitrary finite number of internal channels and any geometry of their location in the MOF cross-section is proposed. It is assumed that the outer boundary of the MOF and the channel boundaries are closed and described by arbitrary single-valued functions of the angular variables $\rho_0(\varphi)$ and $\rho_k(\varphi_k)$ in global and local coordinate systems. The longitudinal components of the mode electromagnetic field at the indicated boundaries are represented by Fourier polynomials in angular variables. With the use of two-dimensional Green's functions for each of the homogeneous media forming MOFs and the representation of these functions by series in cylindrical functions, based on the Graf addition theorem, the homogeneous algebraic system (58) is formulated with respect to the coefficients of the named polynomials. If the functions $\rho_0(\varphi)$ and $\rho_k(\varphi_k)$ have continuous derivatives, then the calculation of the matrix elements of the system involves the integration of continuous functions and does not cause difficulties. The paper presents examples of calculating MOFs with the functions $\rho_0(\varphi)$ and $\rho_k(\varphi_k)$ having the specified property. It is shown that in the particular case of a circular dielectric waveguide the method

gives an exact analytical solution of the waveguide problem. For more complex waveguide structures, such as a dielectric elliptical waveguide and MOF with elliptical air channels, estimates are obtained for the internal convergence of the method with respect to the order of the Fourier polynomials. The modal birefringence in the named MOFs was studied. It was established that the mode dichroism, which consists in the difference in the attenuation coefficients of the main orthogonally polarized modes of these fibers, is significantly affected by the outer boundary of the fiber.

When using waveguide models with discontinuous functions $\rho_0(\varphi)$ and (or) $\rho_k(\varphi_k)$, the calculation of the matrix elements of the system (58) is reduced to the integration of piecewise continuous functions, which also does not cause fundamental difficulties. However, in this case, the Fourier series for the longitudinal components of the mode electromagnetic field are not absolutely convergent. As a result, the described method becomes asymptotic. The manifestation of this feature in the modes calculation of rectangular dielectric waveguides is considered in a separate paper, which will be published in the journal „Bulletin of A.A. Kuleshov Mogilev State University".

Funding

The study was executed under the State Program for Scientific Research of the Republic of Belarus „1.15 Photonics and Electronics for Innovations".

Conflict of interest

The authors declare that they have no conflict of interest.

References

[1] J. Lai, S. Jiang. Appl. Comput. Harmon. Anal., **44** (3), 645 (2018). DOI: 10.1016/j.acha.2016.06.009
[2] W. Lu, Y.Y. Lu. J. Lightwave Technol., **30** (11), 1610 (2012). DOI: 10.1109/JLT.2012.2189355
[3] E. Pone, A. Hassani, S. Lacroix, A. Kabashin, M. Skorobogatiy. Opt. Express, **15** (16), 10231 (2007). DOI: 10.1364/OE.15.010231.
[4] S.V. Boriskina, T.M. Benson, P. Sewell, A.I. Nosich. IEEE J. Sel. Top. Quantum Electron., **8** (6), 1225 (2002). DOI: 10.1109/JSTQE.2002.806729
[5] A.B. Sotsky. *Teoriya opticheskilh volnovodnykh elementov* (UO „MGU im. A.A. Kuleshov", Mogilev, 2011) (in Russian)
[6] T.P. White, B.T. Kuhlmey, R.C. McPhedran, D. Maystre, G. Renversez, C.M. de Sterke, L.C. Botten. J. Opt. Soc. Am. B, **19** (10), 2322 (2002). DOI: 10.1364/JOSAB.19.002322
[7] B.T. Kuhlmey, T.P. White, G. Renversez, D. Maystre, L.C. Botten, C.M. de Sterke, R.C. McPhedran. J. Opt. Soc. Am. B, **19** (10), 2331 (2002). DOI: 10.1364/JOSAB.19.002331
[8] A.B. Sotsky, An Ying. Mogilev State A. Kuleshov University Bull. Ser. B., **59** (1), 42 (2022).
[9] A.B. Sotsky, L.I. Sotskaya, V.P. Minkovich, D. Monzon-Hernandez. Tech. Phys., **54** (6), 865 (2009). https://doi.org/10.1134/S1063784209060152
[10] M.S. Sicacha, V.P. Minkovich, A.B. Sotsky, A.V. Shilov, L.I. Sotskaya, E.A. Chudakov. J. Eur. Opt. Soc.: Rapid Publ., **17**, 24 (2021). DOI: 10.1186/s41476-021-00169-4
[11] D. Marcuse. *Light Transmission Optics* (Van Nostrand Reinhold Company, NY.–Cincinnati–Toronto–London–Melbourne., 1972)
[12] G. Korn, T. Korn. *Mathematical handbook* (McGraw-Hill Book Company, NY.−SF−Toronto−London−Sydney., 1968)
[13] E.A. Ivanov. *Difraktsiya elektromagnitnykh voln yf ldekh telakh* (Nauka, Minsk, 1968) (in Russian)
[14] C. Yeh, F.I. Shimabukuro. *The Essence of Dielectric Waveguides* (Springer, NY., 2008)
[15] D. Marcuse. *Theory of Dielectric Optical Waveguides* (Academic Press, NY., 1974)
[16] M.J. Steel, T.P. White, C.M. de Sterke, R.C. McPhedran, L.C. Botten. Opt. Lett., **26** (8), 488 (2001). DOI: 10.1364/OL.26.000488
[17] A. Snyder, J. Love. *Teoriya opticheskikh volnovodov* (Radio i svyaz, M., 1987) (in Russian)
[18] M.J. Steel, R.M. Osgood. J. Lightwave Technol., **19** (4), 495 (2001). DOI: 10.1109/50.920847
[19] L. Wang, D. Yang. Opt. Express, **15** (14), 8892 (2007). DOI: 10.1364/OE.15.008892
[20] V.P. Minkovich, A.V. Kir'yanov, A.B. Sotsky, L.I. Sotskaya. J. Opt. Soc. Am. B, **21** (6), 1161 (2004). DOI: 10.1364/JOSAB.21.001161
[21] A.B Sotsky, L.I. Sotskaya, O.A. Paushkina. Pis'ma v ZhTF **36**, (10), 81 (2010). (in Russian).
[22] G. Agrawal. *Nonlinear Nelinejnaya volokonnaya optika* (Mir, M., 1996) (in Russian)